J. Am. Chem. Soc. **1993**, *115*, 2465–2472

medium viscosity.[76] Higher ^{1}p* absorbance is observed in the lower viscosity solvents, C_6–C_{16} alkanes, at constant T, and at higher T in the same solvent consistent with the changes of feeding rates of ^{1}p* from ^{1}t*. Kinetics analysis of the evolution of the 351-nm absorption was consistent with a medium-independent lifetime of ^{1}p*-B, $\tau_p = 10 \pm 3$ ps.[76]

In the parent stilbene molecule, an early estimate of $\tau_p = 3 \pm 2$ ps was based on the time evolution of transient absorption at 312.5 nm following excitation of ^1c-d_0.[23a] This was revised downward recently to $\tau_p \leq 0.15$ ps.[23b] Based on our simple mechanism, a rough estimate of τ_p can be obtained by setting $k_{1p} = k_{pl}$. This neglects any possible entropy difference between ^{1}t* and ^{1}p* and, based on the ϕ_{cl} data in Table V, the activation parameters in ref 12 for k_{1p}, and $\tau_p = \phi_{ct}/\alpha_{cp}k_{pl}$, gives $\tau_p = 0.26$ and 0.31 ps for ^{1}p*-d_0 in C_6 and in C_{14}, respectively, at 30 °C. The entry for $\phi_{fl}{}^c$ of ^1c-d_0 in C_6 given in Table V is about 20% larger than the values obtained from flow-cell experiments 1a and 2a. Use of these more reliable values gives $\tau_p = 0.21$ ps at 30 °C. If we assume that the deuterium isotope effect in the ^{1}p$^* \rightarrow {}^1$t* direction is identical with that in the ^{1}t$^* \rightarrow {}^1$p* direction, the same procedure gives $\tau_p = 0.40$ and 0.50 ps for ^1c-d_2 in C_6 and in C_{14}, respectively. This suggests that it should be easier to detect a bottleneck at ^{1}p* in transient decay kinetics of $^1c^*$-d_2. An olefinic-position specific deuterium isotope effect was established previously for the decay of the twisted stilbene triplet, ^{3}p*.[2a,9,77]

The lifetimes inferred for ^{1}p* are very close to the lifetime assigned by Greene et al. to isolated ^{1}c* in the gas phase, $\tau = 0.32$ ps.[78] Since the ^{1}c$^* \rightarrow {}^1$p* process should be barrierless under these conditions, the rate-determining step for the observed transient decay may be the radiationless decay of ^{1}p* to the ground-state surface.

Acknowledgment. This research was supported by NSF Grant CHE 90-14060.

Registry Number supplied by author: **1a**, 17329-15-6.

---

[77] (a) Caldwell, R. A.; Cao, C. V. *J. Am. Chem. Soc.* **1982**, *104*, 6174. (b) Caldwell, R. A. *Pure Appl. Chem.* **1984**, *56*, 1967.

[78] Greene, B. I.; Farrow, R. C. *J. Chem. Phys.* **1983**, *78*, 3336.

Tautomeric Equilibrium and Hydrogen Shifts of Tetrazole in the Gas Phase and in Solution

Ming Wah Wong,* Regis Leung-Toung, and Curt Wentrup*

Contribution from the Chemistry Department, The University of Queensland, Brisbane, Queensland 4072, Australia.
Received October 5, 1992

Abstract: High-level ab initio molecular orbital calculations, using basis sets up to 6-311+G(2d,2p) with electron correlation incorporated at the quadratic configuration interaction [QCISD(T)] level, have been used to study the tautomeric equilibrium and hydrogen shifts of tetrazole in the gas phase and in solution. The solvent effects were investigated by self-consistent reaction field (SCRF) theory. Consistent with experimental observations, the 1*H*-tetrazole (**1**)/2*H*-tetrazole (**2**) tautomeric equilibrium is calculated to be strongly influenced by the surrounding medium. 2*H*-Tetrazole is the energetically preferred tautomer in the gas phase. In a nonpolar solution, both the 1*H* and 2*H* forms are predicted to exist in comparable amounts. However, in a medium of high dielectric constant the more polar 1*H* tautomer is the dominant species. The calculated free energy changes for tautomerization of 1*H*-tetrazole in the gas phase and in nonpolar ($\epsilon = 2$) and polar ($\epsilon = 40$) media are −7, 1, and 12 kJ mol^{-1}, respectively. The molecular geometry, charge distribution, and vibrational frequencies of the polar 1*H* tautomer are found to be altered significantly in the presence of a solvent reaction field. Isomerization of **1** to **2**, via a [1,2] hydrogen shift, requires an energy barrier of 207 kJ mol^{-1} in the gas phase. 5*H*-Tetrazole (**3**) is predicted to lie 82 kJ mol^{-1} above **1**, due to its nonaromatic character. However, rearrangement of **3** to **1**, via a [1,5] hydrogen shift, is inhibited by an activation barrier of 150 kJ mol^{-1}. Conversely, the energy barrier for the rearrangement of **1** to **3** is 232 kJ mol^{-1}, slightly larger than that required for the isomerization of **1** to **2**. These results suggest that **3** is a good candidate for experimental observation. Inclusion of electron correlation leads to a drastic change in the molecular geometry of **3**. At the MP2 level, an acyclic structure is predicted, while at the MP3 and QCISD levels the expected cyclic structure is found. The calculated molecular geometry of 1*H*-tetrazole at the MP2 level is found to differ significantly from the available solid-state structural data.

Introduction

There has been considerable and continuing interest in the chemistry of tetrazoles.[1] In principle, three protomers of unsubstituted tetrazole are possible, namely 1*H*- (**1**), 2*H*- (**2**), and 5*H*-tetrazole (**3**) (Figure 1). Both **1** and **2** have been observed experimentally.[2-6] Results from X-ray crystallography unambiguously showed that tetrazole exists as the 1*H* tautomer (**1**) in the solid state.[2] In solution, there is an equilibrium between **1**

---

[1] (a) Benson, F. R. In *Heterocyclic Compounds*; Elderfield, R. C., Ed.; Wiley: New York, 1967; Vol. 8. (b) Grimmett, M. R. *Comprehensive Organic Chemistry*; Pergamon Press: New York, 1979; Vol. 4. (c) Butler, R. N. In *Comprehensive Heterocyclic Chemistry*; Katritzky, A. R., Rees, C. W., Eds.; Pergamon Press: New York, 1984; Vol. 5.

[2] van der Putten, N.; Heijdenrijk, D.; Schenk, H. *Cryst. Struct. Commun.* **1974**, 321.

[3] (a) Wofford, D. S.; Forkey, D. M.; Russell, J. G. *J. Org. Chem.* **1982**, *47*, 5132. (b) Charton, M. *J. Chem. Soc. B* **1969**, 1240. (c) Witanowski, M.; Stefaniak, L.; Januszewski, H.; Grabowski, Z.; Webb, G. A. *Tetrahedron* **1972**, *28*, 637. (d) Moore, D. G. W.; Whittaker, A. G. *J. Am. Chem. Soc.* **1960**, *82*, 5007. (e) Kaufman, M. H.; Ernsberger, F. M.; Ewans, W. S. *J. Am. Chem. Soc.* **1956**, *78*, 4197. (f) Henry, R. A. *J. Am. Chem. Soc.* **1951**, *73*, 4470. (g) Jensen, K. A.; Fredgier, A. K. *Dan. Vidensk. Selsk., Mat.-Fys. Medd.* **1943**, *20*, 1.

[4] Krugh, W. D.; Gold, L. P. *J. Mol. Spectrosc.* **1974**, *49*, 423.

0002-7863/93/1515-2465$04.00/0

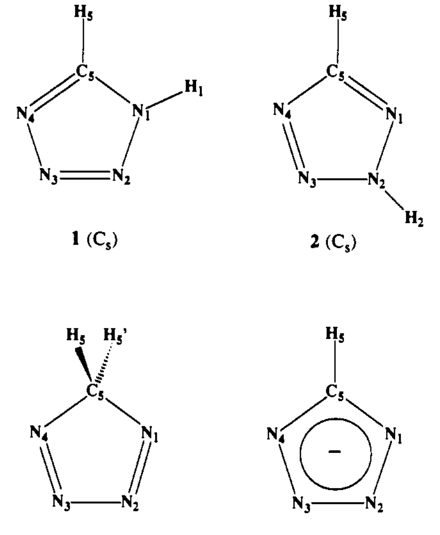

1 (C_s) 2 (C_s)

3 (C_{2v}) 6 (C_{2v})

Figure 1. Equilibrium structures of tetrazole (**1**, **2**, and **3**) and tetrazole anion (**6**).

and **2** which is found to be very sensitive to the solvent as well as to the nature of the substituents.[1,3] Consequently, much effort, both experimental and theoretical, has been devoted to the study of tetrazole tautomerism in the gas phase.[4-7] Earlier microwave[4] and mass spectroscopic[5] studies indicated that both 1*H* and 2*H* forms are present in the gas phase. However, strong photoelectron spectroscopic evidence for the preference of the 2*H* tautomer **2** in the gas phase has recently been published.[6] The experimental conclusion was supported by theoretical calculations.[6,7] Previous semiempirical and ab initio studies indicated that the two tautomeric forms are similar in energy, with a slight preference for the less polar 2*H* form. However, a recent MRCI study suggested that the 2*H* tautomer is more stable than the 1*H* form by 99 kJ mol^{-1}![7e]

Recent experimental studies have demonstrated the formation of nitrilimines II on both flash vacuum pyrolysis (FVP) and matrix photolysis of 2,5-disubstituted tetrazoles I.[8] Furthermore, we find that 5-monosubstituted tetrazoles I (R' = H; R = aryl) give rise to diazo compounds III in ca. 10% isolated yields together with cyanamides (R—NH—CN) and monosubstituted carbodiimides (R—N=C=HN).[9] Diazomethane has also been detected, together with cyanamide, in the FVP of tetrazole.[7d] The question arises, therefore, whether nitrilimines II (R' = H) can isomerize to diazo compounds III[9,10] or whether the latter are a consequence of an initial [1,5] hydrogen shift[11] to the unknown 5*H*-tetrazole IV (Scheme I).

Scheme I

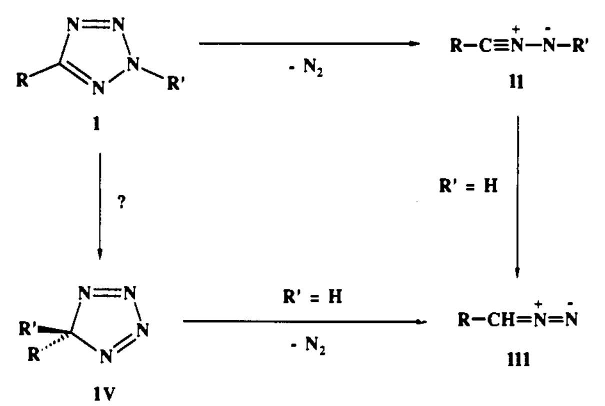

Our goals in the present paper are 2-fold. Firstly, we investigate the 1*H*-tetrazole/2*H*-tetrazole tautomeric equilibrium in the gas phase and in solution. The effect of solvent is calculated by Onsager's reaction field model,[12] as implemented in the context of ab initio molecular orbital (MO) theory.[13,14] This method has been applied successfully to study several solvent effect problems.[13,15] In particular, the solvent effect on the 2-pyridone/2-hydroxypyridine tautomeric equilibrium was well reproduced by the reaction field theory.[15c] Secondly, we use high-level ab initio theory to examine the possible hydrogen shifts connecting 1*H*- (**1**), 2*H*- (**2**), and 5*H*-tetrazole (**3**). We wish to determine whether the unknown 5*H* isomer is a potentially observable and energetically accessible species.

Theoretical Methods and Results

Standard ab initio molecular orbital calculations[16] were carried out with the GAUSSIAN 90[17] and GAUSSIAN 92[18] series of programs. Geometry optimizations for all structures were carried out with the 6-31G* basis set[16] at the Hartree–Fock (HF) level with $\epsilon = 1$ (corresponding to the gas phase), $\epsilon = 2$ (representing nonpolar solution), and $\epsilon = 40$ (representing polar medium). Harmonic vibrational frequencies and infrared intensities were predicted at these equilibrium geometries. The directly calculated zero-point vibrational energies (ZPVEs) were scaled by 0.89 to account for the overestimation of vibrational frequencies at the HF level.[19] Improved relative energies were obtained through

---

(5) Forkey, D. M.; Carpenter, W. R. *Org. Mass Spectrom.* **1969**, *2*, 433.

(6) (a) Razynska, A.; Tempczyk, A.; Maslinski, E.; Szafranek, J.; Grzonka, Z. *J. Chem. Soc., Perkin Trans. 2* **1983**, 379. (b) Palmer, M. H.; Simpson, I.; Wheeler, J. R. *Z. Naturforsch.* **1981**, *36A*, 1246.

(7) (a) Lesnikovich, A. I.; Ivashkevich, O. A.; Printsev, G. V.; Gaponik, P. N.; Levchik, S. V. *Thermochim. Acta* **1990**, *171*, 207. (b) Fabian, W. M. F. *Z. Naturforsch. A: Phys. Sci.* **1990**, *45*, 1328. (c) Kozyro, A. A.; Simirskii, V. V.; Krasulin, A. P.; Sevruk, V. M.; Kabo, G. Y.; Frenkel, M. L.; Gaponik, P. N.; Grigor'ev, Y. V. *Zh. Fiz. Khim.* **1990**, *64*, 656. (d) Guimon, C.; Khayar, S.; Gracian, F.; Begtrup, M.; Pfister-Guillouzo, G. *Chem. Phys.* **1989**, *138*, 157. (e) Palmer, M. H.; Beveridge, A. J. *Chem. Phys.* **1987**, *111*, 249. (f) Mo, O.; de Paz, J. L. G.; Yanez, M. *J. Phys. Chem.* **1986**, *90*, 5597. (g) Mazurek, A. P.; Osman, R. *J. Phys. Chem.* **1985**, *89*, 460. (h) Fos, E.; Vilarrosa, J.; Fernandez, J. *J. Org. Chem.* **1985**, *50*, 4894. (i) Catalan, J.; de Paz, J. L. G.; Yanez, M.; Elguero, J. *Chem. Scripta* **1984**, *24*, 84. (j) Lumbroso, H.; Liegeois, C.; Pappalarado, G. C.; Grassi, A. *J. Mol. Struct.* **1982**, *82*, 283.

(8) (a) Wentrup, C.; Fischer, S.; Maquestiau, A.; Flammang, R. *Angew. Chem., Int. Ed. Engl.* **1985**, *24*, 56. (b) Bock, H.; Dammel, R.; Fischer, S.; Wentrup, C. *Tetrahedron Lett.* **1987**, *28*, 619. (c) Toubro, N. H.; Holm, A. *J. Am. Chem. Soc.* **1980**, *102*, 2093. (d) Meier, H.; Heinzelmann, W.; Heimgartner, H. *Chimia* **1980**, *34*, 504, 506.

(9) (a) Wentrup, C. *Helv. Chim. Acta* **1978**, *61*, 1755. (b) Gleiter, R.; Rettig, W.; Wentrup, C. *Ibid.* **1974**, *57*, 2111. (c) Fischer, S.; Qiao, G. G.; Wentrup, C., unpublished results. (d) Fischer, S. Ph.D. Thesis, The University of Marburg, Germany, 1985.

(10) (a) For a suggested nitrilimine-to-diazo compound isomerization in the FVP of 2,4-disubstituted-1,3,4-oxadiazolin-5-ones, see: Padwa, A.; Caruso, T.; Nahm, S.; Rodriguez, A. *J. Am. Chem. Soc.* **1982**, *104*, 2865. (b) For the isomerization of *N*-silyl and *N*-phosphanyl nitrilimines to diazo compounds, see: Granier, M.; Baceiredo, A.; Bertrand, G. *Angew. Chem., Int. Ed. Engl.* **1988**, *27*, 1350. (c) Granier, M.; Baceiredo, A.; Grutzmacher, H.; Pritzkow, H.; Bertrand, G. *Ibid.* **1990**, *29*, 659. (d) For the nonoccurrence of such migrations, see: Reau, R.; Veneziani, G.; Bertrand, G. *J. Am. Chem. Soc.* **1992**, *114*, 6059.

(11) (a) Hoffmann, R.; Woodward, R. B. *J. Am. Chem. Soc.* **1965**, *87*, 395. (b) Woodward, R. B.; Hoffmann, R. *Ibid.* **1965**, *87*, 2511.

(12) Onsager, L. *J. Am. Chem. Soc.* **1936**, *58*, 1486.

(13) Wong, M. W.; Frisch, M. J.; Wiberg, K. B. *J. Am. Chem. Soc.* **1991**, *113*, 4776.

(14) Tapia, O.; Goscinski, O. *Mol. Phys.* **1975**, *29*, 1653.

(15) (a) Wong, M. W.; Wiberg, K. B.; Frisch, M. J. *J. Chem. Phys.* **1991**, *89*, 8991. (b) Wong, M. W.; Wiberg, K. B.; Frisch, M. J. *J. Am. Chem. Soc.* **1992**, *114*, 523. (c) Wong, M. W.; Wiberg, K. B.; Frisch, M. J. *J. Am. Chem. Soc.* **1992**, *114*, 1645. (d) Wiberg, R. B.; Wong, M. W. *J. Am. Chem. Soc.*, in press. (e) Foresman, J. B.; Wong, M. W.; Wiberg, K. B.; Frisch, M. J. *J. Am. Chem. Soc.*, in press.

(16) Hehre, W. J.; Radom, L.; Schleyer, P. v. R.; Pople, J. A. *Ab Initio Molecular Orbital Theory*; Wiley: New York, 1986.

(17) Frisch, M. J.; Head-Gordon, M.; Trucks, G. W.; Foresman, J. B.; Schlegel, H. B.; Raghavachari, K.; Robb, M. A.; Binkley, J. S.; Gonzalez, C.; DeFrees, D. J.; Fox, D. J.; Whiteside, R. A.; Seeger, R.; Melius, C. F.; Baker, J.; Martin, R. L.; Kahn, L. R.; Stewart, J. J. P.; Topiol, S.; Pople, J. A. *GAUSSIAN 90*; Gaussian Inc.: Pittsburgh, PA, 1990.

(18) Frisch, M. J.; Trucks, G. W.; Head-Gordon, M.; Gill, P. M. W.; Wong, M. W.; Foresman, J. B.; Johnson, B. G.; Schlegel, H. B.; Robb, M. A.; Replogle, E. S.; Gomperts, R.; Andres, J. L.; Raghavachari, K.; Binkley, J. S.; Gonzalez, C.; Martin, R. L.; Fox, D. J.; DeFrees, D. J.; Baker, J.; Stewart, J. J. P.; Pople, J. A. *GAUSSIAN 92*; Gaussian Inc.: Pittsburgh, PA, 1992.

Table I. Calculated Total Energies[a,b] (hartrees) and Relative Energies[c] (kJ mol^{-1}) of 1*H*- and 2*H*-tetrazole

level	total energy		relative energy
	1*H*-tetrazole	2*H*-tetrazole	
HF/STO-3G[d]	−253.472 08	−253.472 73	−1.7
HF/3-21G[d]	−255.268 76	−255.267 18	4.1
HF/6-31G*[d]	−256.754 08	−256.757 04	−7.8
MP2/6-31G*[d]	−257.554 43	−257.560 55	−16.1
HF/6-311G**	−256.806 00	−256.808 76	−7.2
MP2/6-311G**	−257.642 60	−257.649 29	−17.6
MP3/6-311G**	−257.634 01	−257.638 81	−12.6
MP4/6-311G**	−257.696 01	−257.700 83	−12.7
QCISD/6-311G**	−257.646 12	−257.650 05	−10.3
QCISD(T)/6-311G**	−257.687 57	−257.691 89	−11.3
HF/6-311+G(2d,2p)	−256.821 57	−256.823 70	−5.6
MP2/6-311+G(2d,2p)	−257.709 49	−257.715 31	−15.3
QCISD(T)/6-311+G(2d,2p)	−257.754 47	−257.757 91	−9.0
HF/6-311+G(3df,2p)	−256.835 72	−256.837 53	−4.8
MP2/6-311+G(3df,2p)	−257.806 30	−257.812 21	−15.5
G1[e]	−257.920 82	−257.924 80	−10.4
G2[e]	−257.921 90	−257.925 40	−9.2
G2[f]	−257.875 51	−257.878 48	−7.8

[a] Based on MP2/6-31G* optimized geometries, unless otherwise noted. [b] All total energies at correlated level (except MP2/6-31G*) refer to frozen-core calculations. [c] E(2*H*-tetrazole) − E(1*H*-tetrazole). [d] Using fully optimized geometries. [e] E_e values. [f] Include zero-point vibrational corrections (i.e., E_0 values).

second-order Møller–Plesset (MP2)[20] calculations with the larger 6-311+G** basis set[16] based on the HF/6-31G* optimized geometries.

For the gas-phase equilibrium and transition structures, additional optimizations and frequency calculations were performed at the MP2/6-31G* level. Higher-level energy calculations were computed at the quadratic configuration interaction with singles, doubles, and augmented triples (QCISD(T))[21] level with the 6-311+G(2d,2p) basis set,[16] using the MP2/6-31G* optimized geometries (except for 5*H*-tetrazole, see reason below). This level of theory is evaluated with the use of the additivity approximation,

$$\Delta E(\text{QCISD(T)/6-311+G(2d,2p)}) = \Delta E(\text{QCISD(T)/6-311G**}) - \Delta E(\text{MP2/6-311G**}) + \Delta E(\text{MP2/6-311+G(2d,2p)}) \quad (1)$$

Our best gas-phase relative energies correspond to the QCISD(T)/6-311+G(2d,2p) level together with zero-point energy contributions (MP2/6-31G*). Unless otherwise noted, these are the values given in the text. To investigate the effect of basis set and electron correlation on the tautomerization energy of 1*H*-tetrazole in the gas phase, we have performed single-point energy calculations at the HF level with a hierarchy of basis sets:[16] STO-3G, 3-21G, 6-31G*, 6-311G**, 6-311+G(2d,2p), 6-311+G(3df,2p); MP2, MP3, MP4, QCISD and QCISD(T) levels[20,21] with the 6-311G** basis set; and G1 and G2 theories.[22,23]

The effect of solute–solvent interaction was calculated by the self-consistent reaction field (SCRF) method,[13] which is based on Onsager's reaction field theory of electrostatic solvation.[12] In the reaction field model, the solvent is treated as a dielectric continuum (ϵ). The solute is assumed to occupy a spherical cavity of radius a_0 in the medium. The electrostatic contribution from the solvent leads to an energetic stabilization of the solute dipole. In the SCRF MO formalism, the solute–solvent interaction is treated as a perturbation of the Hamiltonian of the isolated molecule. The reaction field is updated iteratively until a self-consistency is achieved for the intramolecular electric field.[13] The solvation energy calculated by the SCRF method corresponds to the electrostatic contribution to the free energy of solvation. In the present work, the cavity radius (a_0 = 3.45 Å) of tetrazole was calculated by a quantum mechanical approach,[24] which involves computing the molecular volume of the 0.001-au electron density envelope (based on the HF/6-31G** wave function) and scaling by 1.33 to obtain an estimate of the molar volume in the liquid phase. An increment of 0.5 Å was added to the final a_0 value to account for the nearest approach of solvent molecules. Since tetrazole is a relatively compact molecule, the simple spherical approximation is a satisfactory approximation. Note that the calculated (scaled) molecular volume of tetrazole (47 cm^3 mol^{-1}) is in very good agreement with the experimental molar volume in the crystalline state (48 cm^3 mol^{-1}).[2]

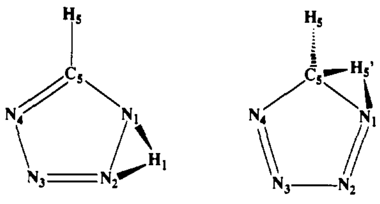

4 (C_1) 5 (C_1)

Figure 2. Transition structures for [1,2] hydrogen shift from **1** to **2** (**4**) and for [1,5] hydrogen shift from **1** to **3** (**5**).

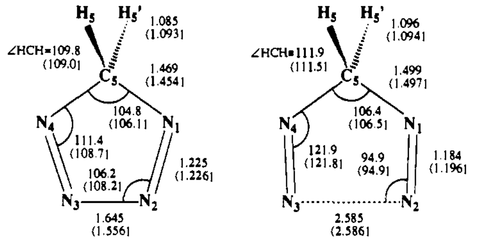

3 (a) **3** (b)

Figure 3. Optimzied geometry of 5*H*-tetrazole (**3**): (a) cyclic (QCISD/6-31G*, with MP3/6-31G* values in parentheses) and (b) open (MP2/6-311G(2d,2p), with MP2/6-31G* values in parentheses).

The charge distributions of the tetrazole isomers in the gas and liquid phases were examined by Bader's theory of atoms in molecules,[25] in which the electron population for a given atom is integrated over a well-defined volume element. The charge densities were obtained from the HF/6-31+G** calculations based on the HF/6-31G* optimized geometries. The analysis of the wave functions was carried out with PROAIM program.[26]

Calculated total and relative energies in the gas phase are given in Tables I and II. Calculated entropies, enthalpies, zero-point vibrational energies, free energies, thermal corrections, and dipole moments are summarized in Tables III and IV. Equilibrium and transition structures of tetrazole are shown in Figures 1–3, and their optimized structural parameters are collected in Tables V–VII. Vibrational frequencies and infrared intensities of all tetrazole isomers are presented in Table VIII. Finally, the calculated electron populations are given in Table IX. Throughout this paper, bond lengths are given in angstroms and bond angles in degrees.

Tautomeric Equilibrium

The theoretical prediction of the tautomerization energy of tetrazole in the gas phase has been the subject of intense interest in the past decade.[7] Most ab initio calculations to date suggested that the 2*H* tautomer **2** is favored over the 1*H* form **1** by about 5–10 kJ mol^{-1}. However, a considerably larger energy difference (99 kJ mol^{-1}) has been reported in a recent MRCI study.[7e] Here we attempt to establish a more definitive theoretical estimate of the relative energy by considering the effect of basis set and electron correlation in greater detail (Table I). As noted before,[7f,g,i] the calculated energy difference (ΔE) between 1*H*- (**1**) and 2*H*-tetrazole (**2**) is somewhat misleading at low levels of theory, i.e., there is a reversal of the stability of **1** relative to **2** at the HF/3-21G level. At the HF/6-31G* level, **2** is calculated to be more stable than **1** by 8 kJ mol^{-1}. Further improvement of basis set at the HF level (from 6-31G* → 6-311+G(3df,2p)) lowers the

---

(19) (a) Pople, J. A.; Schlegel, H. B.; Raghavachari, K.; DeFrees, D. J.; Binkley, J. S.; Frisch, M. J.; Whitesides, R. F.; Hout, R. F.; Hehre, W. J. *Int. J. Quantum Chem. Symp.* **1981**, *15*, 269. (b) DeFrees, D. J.; McLean, A. D. *J. Chem. Phys.* **1985**, *82*, 333.

(20) (a) Møller, C.; Plesset, M. S. *Phys. Rev.* **1934**, *46*, 618. (b) Pople, J. A.; Binkley, J. S.; Seeger, R. *Int. J. Quantum Chem. Symp.* **1976**, *10*, 1.

(21) Pople, J. A.; Head-Gordon, M.; Raghavachari, K. *J. Chem. Phys.* **1987**, *87*, 5968.

(22) Curtiss, L. A.; Jones, C.; Trucks, G. W.; Raghavachari, K.; Pople, J. A. *J. Chem. Phys.* **1990**, *93*, 2537.

(23) Curtiss, L. A.; Raghavachari, K.; Trucks, G. W.; Pople, J. A. *J. Chem. Phys.* **1991**, *94*, 7221.

(24) Wong, M. W.; Wiberg, K. B.; Frisch, M. J. *J. Phys. Chem.*, submitted for publication.

(25) (a) Bader, R. F. W. *Acc. Chem. Res.* **1985**, *18*, 9. (b) Bader, R. F. W. *Atoms in Molecules. A Quantum Theory*; Oxford University Press: New York, 1990.

(26) Biegler-Konig, F. W.; Bader, R. F. W.; Tang, T.-H. *J. Comput. Chem.* **1982**, *3*, 317.

Table II. Calculated Total Energies[a] (hartrees), Zero-Point Vibrational Energies[b] (ZPVE, kJ mol^{-1}), and Relative Energies (kJ mol^{-1}) in the Gas Phase

level	1H-tetrazole (**1**)	2H-tetrazole (**2**)	5H-tetrazole (**3**)	T.S. (**4**): **1** → **2**	T.S. (**5**): **1** → **3**
		Total Energy			
HF/6-31G*[c]	−256.754 08	−256.757 04	−256.714 50	−256.646 83	−256.644 37
MP2/6-31G*	−257.554 43	−257.560 55	−257.524 01	−257.469 73	−257.458 27
MP2/6-311G**[d]	−257.642 60	−257.649 29	−257.599 26[e]	−257.562 52	−257.548 72
MP2/6-311+G(2d,2p)[d]	−257.709 50	−257.715 31	−257.665 78[e]	−257.628 33	−257.615 47
QCISD(T)/6-311G**[d]	−257.687 57	−257.691 89	−257.654 76[e]	−257.604 25	−257.594 14
QCISD(T)/6-311+G(2d,2p)[f]	−257.754 47	−257.757 91	−257.721 19[e]	−257.670 06	−257.660 89
ZPVE	121.40	122.78	116.39	106.44	107.82
		Relative Energy			
HF/6-31G*	0.0	−7.8	103.9	281.6	288.0
MP2/6-31G*	0.0	−16.1	79.9	222.4	252.5
MP2/6-311G**	0.0	−17.6	113.8	210.3	283.6
MP2/6-311+G(2d,2p)	0.0	−15.3	114.8	213.1	246.9
QCISD(T)/6-311G**	0.0	−11.3	86.4	218.8	245.3
QCISD(T)/6-311+G(2d,2p)	0.0	−9.0	87.4	221.6	245.7
QCISD(T)/6-311+G(2d,2p)[g]	0.0	−7.7	82.4	206.7	232.1

[a] Based on MP2/6-31G* optimized geometries, unless otherwise noted. [b] HF/6-31G* values; scaled by 0.89. [c] HF/6-31G* optimized geometries. [d] Frozen-core approximation. [e] QCISD/6-31G* optimized geometries. [f] Evaluated from additivity scheme, see text. [g] Include zero-point vibrational corrections.

Table III. Calculated Energies[a,b] and Dipole Moments[c] (μ) in the Gas Phase ($\epsilon = 1$) and in Solutions ($\epsilon = 2$ and $\epsilon = 40$)

	$\epsilon = 1$	$\epsilon = 2$	$\epsilon = 40$
	1H-Tetrazole (**1**)		
E(HF/6-31G*)	−256.754 08	−256.757 83	−256.763 87
E(HF/6-311+G**)	−256.821 21	−256.825 10	−256.831 50
E(MP2/6-311+G**)	−257.647 66	−257.651 50	−257.657 17
ZPVE	136.41	136.63	136.90
S[d]	266.19	266.01	265.77
$H - H_0$	11.65	11.61	11.54
μ	5.58	5.95	6.56
	2H-Tetrazole (**2**)		
E(HF/6-31G*)	−256.757 04	−256.757 66	−256.758 65
E(HF/6-31+G**)	−256.824 36	−256.824 98	−256.826 01
E(MP2/6-311+G**)	−257.654 05	−257.654 76	−257.655 94
ZPVE	137.95	137.97	138.00
S[d]	265.49	265.44	265.36
$H - H_0$	11.49	11.48	11.46
μ	2.43	2.59	2.85
	5H-Tetrazole (**3**)		
E(HF/6-31G*)	−256.714 50	−256.715 78	−256.717 84
E(HF/6-311+G**)	−256.778 66	−256.779 98	−256.782 20
E(MP2/6-311+G**)	−257.600 28	−257.601 58	−257.603 68
ZPVE	130.77	130.73	130.66
S[d]	269.51	269.51	269.50
$H - H_0$	12.22	12.22	12.22
μ	3.28	3.50	3.86
	T.S. (**4**): **1** → **2**		
E(HF/6-31G*)	−256.646 83	−256.647 92	−256.649 66
E(HF/6-311+G**)	−256.717 67	−256.718 77	−256.720 57
E(MP2/6-311+G**)	−257.565 79	−257.566 87	−257.568 63
ZPVE	119.60	119.57	119.51
S[d]	265.18	265.18	265.18
$H - H_0$	11.37	11.37	11.37
μ	2.98	3.16	3.47
	T.S. (**5**): **1** → **3**		
E(HF/6-31G*)	−256.644 37	−256.646 39	−256.649 64
E(HF/6-311+G**)	−256.712 77	−256.714 85	−256.718 32
E(MP2/6-311+G**)	−257.553 29	−257.555 18	−257.558 32
ZPVE	121.15	121.14	121.09
S[d]	264.57	264.57	264.56
$H - H_0$	11.19	11.18	11.18
μ	4.02	4.29	4.74

[a] Based on HF/6-31G* geometries. [b] E in hartrees; ZPVE and $H - H_0$ in kJ mol^{-1}; S in J mol^{-1} K^{-1}. [c] MP2/6-311+G** values; in D. [d] The solution entropies were calculated using the gas-phase translational partition coefficient.

Table IV. Calculated Relative Free Energies (ΔG)[a,b]

	$\epsilon = 1$	$\epsilon = 2$	$\epsilon = 40$
2H-Tetrazole (**2**)			
ΔE(HF/6-31G*)	−7.77	0.45	13.71
ΔE(HF/6-311+G**)	−8.27	0.32	14.41
ΔE(MP2/6-311G**)	−16.78	−8.17	3.23
ΔE(QCISD(T)/6-311+G(2d,2p)[c]	−9.03	−0.81	10.97
ΔH[d,e]	−7.65	0.41	11.99
ΔG[f]	−7.44	0.58	12.11
5H-Tetrazole (**3**)			
ΔE(HF/6-31G*)	103.92	110.40	120.85
ΔE(HF/6-311+G**)	111.72	118.46	129.44
ΔE(MP2/6-311+G**)	124.40	131.06	140.44
ΔE(QCISD(T)/6-311+G(2d,2p)[c]	87.38	94.05	103.42
ΔH[d,e]	82.31	88.77	97.86
ΔG[f]	81.32	87.72	96.74
T.S. (**4**): **1** → **2**			
ΔE(HF/6-31G*)	281.58	288.57	299.86
ΔE(HF/6-311+G**)	271.84	279.17	291.25
ΔE(MP2/6-311+G**)	214.95	222.20	232.46
ΔE(QCISD(T)/6-311+G(2d,2p)[c]	221.62	228.86	239.13
ΔH[d,e]	204.52	211.57	221.56
ΔG[f]	204.82	211.82	221.74
T.S. (**5**): **1** → **3**			
−ΔE(HF/6-31G*)	288.04	292.59	299.91
ΔE(HF/6-311+G**)	284.71	289.46	297.15
ΔE(MP2/6-311+G**)	247.77	252.89	259.33
ΔE(QCISD(T)/6-311+G(2d,2p)[c]	245.96	251.08	257.73
ΔH[d,e]	230.23	235.17	241.55
ΔG[f]	230.72	235.60	241.91

[a] Relative to 1H-tetrazole (**1**); ΔE, ΔH, and ΔG in kJ mol^{-1}. [b] At room temperature (T = 298 K), calculated from energy data in Tables II and III. [c] ΔE(QCISD(T)) for $\epsilon = 2$ and 40 were estimated from the gas-phase ΔE(QCISD(T)) values together with the solvation energies calculated at the MP2/6-311+G** level (see text). [d] Based on ΔE calculated at the QCISD/6-311+G(2d,2p) level. [e] $\Delta H = \Delta E + \Delta$(ZPVE) $+ \Delta(H - H_0)$. [f] $\Delta G = \Delta H - T\Delta S$.

calculated energy difference to −5 kJ mol^{-1}. Interestingly, a similar improvement of basis set at the MP2 level leads to a smaller change in ΔE (−0.5 kJ mol^{-1}). To investigate the effect of electron correlation, we have calculated the tautomerization energy of 1H-tetrazole (ΔE) with MP2, MP3, MP4, QCISD, and QCISD(T) methods using the 6-311G** basis set (Table I). The most advanced method considered is QCISD(T). Improvements in the level of electron correlation result in an increase in the energy difference, which appears to be converging on −11 mol^{-1}. The MP2 relative energy overestimates the ΔE, while higher treatments of electron correlation at the MP3, MP4, and QCISD levels are close to the QCISD(T) value. The effect of triple substitutions at the QCISD(T) level is small. At our best level of theory, Gaussian-2 (corresponding effectively to the QCISD(T)/6-311+G(3df,2p) level with isogyric correction), 2H-tetrazole is

Table V. Optimized Structural Parameters for the Equilibrium Structures of Tetrazole and Tetrazole Anion

	gas phase		solution[a,b]	
parameter	HF/6-31G*	MP2/6-31G*	$\epsilon = 2$	$\epsilon = 40$
	1*H*-Tetrazole (**1**)			
$r(C_5{-}N_1)$	1.330	1.347	−0.001	−0.002
$r(C_5{-}N_4)$	1.289	1.325	0.001	0.004
$r(N_1{-}N_2)$	1.326	1.347	−0.001	−0.003
$r(N_2{-}N_3)$	1.252	1.321	0.001	0.002
$r(N_3{-}N_4)$	1.341	1.362	0.000	−0.001
$r(C_5{-}H_5)$	1.068	1.079	0.000	0.000
$r(N_1{-}H_1)$	0.994	1.014	0.001	0.003
$\angle N_1C_5N_4$	108.17	108.22	−0.03	−0.10
$\angle C_5N_1N_2$	108.02	109.50	0.07	0.20
$\angle C_5N_4N_3$	105.77	106.00	−0.05	−0.08
$\angle N_1N_2N_3$	106.68	105.34	0.00	0.00
$\angle N_4N_3N_2$	111.37	110.94	−0.01	−0.03
$\angle H_5C_5N_1$	125.03	124.97	−0.09	−0.22
$\angle H_1N_1C_5$	131.22	130.76	−0.23	−0.58
	2*H*-Tetrazole (**2**)			
$r(C_5{-}N_1)$	1.300	1.344	0.000	0.000
$r(C_5{-}N_4)$	1.344	1.349	0.000	−0.001
$r(N_1{-}N_2)$	1.308	1.326	−0.001	−0.002
$r(N_2{-}N_3)$	1.291	1.339	0.001	0.002
$r(N_3{-}N_4)$	1.276	1.333	0.001	0.002
$r(C_5{-}H_5)$	1.067	1.079	0.000	0.000
$r(N_2{-}H_2)$	0.995	1.016	0.000	0.001
$\angle N_1C_5N_4$	112.05	113.52	0.00	−0.01
$\angle C_5N_1N_2$	101.13	99.92	0.03	0.08
$\angle C_5N_4N_3$	105.97	106.22	−0.03	−0.07
$\angle N_1N_2N_3$	114.30	115.85	−0.01	−0.02
$\angle N_4N_3N_2$	106.50	104.50	0.01	0.02
$\angle H_5C_5N_1$	124.03	122.64	−0.05	−0.14
$\angle H_2N_2N_1$	123.26	122.40	−0.06	−0.18
	5*H*-Tetrazole (**3**)			
$r(C_5{-}N_1)$	1.442	1.497	0.000	0.001
$r(N_1{-}N_2)$	1.206	1.196	0.000	0.000
$r(N_2{-}N_3)$	1.472	2.191	0.000	−0.001
$r(C_5{-}H_5)$	1.082	1.093	0.000	0.000
$\angle N_1C_5N_4$	103.64	106.49	−0.05	−0.15
$\angle C_5N_1N_2$	108.95	121.71	0.04	0.08
$\angle N_1N_2N_3$	109.22	94.94	−0.02	−0.03
$\angle H_5C_5N_1$	110.87	109.71	0.04	0.11
$\angle H_5C_5H_5'$	109.62	111.48	−0.10	−0.29
	Tetrazole Anion (**6**)			
$r(C_5{-}N_1)$	1.317	1.345	0.000	0.000
$r(N_1{-}N_2)$	1.322	1.359	0.000	−0.001
$r(N_2{-}N_3)$	1.284	1.347	0.000	0.001
$r(C_5{-}H_5)$	1.073	1.085	0.000	−0.001
$\angle N_1C_5N_4$	112.34	113.75	−0.03	−0.12
$\angle C_5N_1N_2$	103.75	103.67	0.03	0.09
$\angle N_1N_2N_3$	110.03	109.46	−0.01	−0.03
$\angle H_5C_5N_1$	123.78	123.12	0.02	0.06

[a] SCRF calculations ($a_0 = 3.45$ Å). [b] Change from the gas phase to solution (HF/6-31G*).

more stable than 1*H*-tetrazole by 9 kJ mol^{-1}. Zero-point correction leads to our final and best value of −8 kJ mol^{-1}. This result is in good accord with the experimental conclusion, from microwave,[4] photoelectron,[6] and mass spectroscopy,[5] that the 2*H*-tetrazole is the preferred tautomer in the gas phase.[5,6] Note that our calculated energy differences between and **1** and **2** at various levels of theory (Table I) are all considerably smaller than the MRCI value (99 kJ mol^{-1}) reported by Palmer and Beveridge.[7e] It thus appears that the MRCI value overestimates the relative energy. This conclusion is further supported by the fact that both tautomeric forms are observed in the gas phase.[4,5]

Table VI. Calculated and Experimental Geometry of 1*H*-Tetrazole

	gas phase		condensed phase		
parameter	MP2[a]	QCISD[b]	SCRF[c]	dimer[d]	expt[e]
$r(C_5{-}N_1)$	1.345	1.348	−0.003	−0.003	1.33
$r(C_5{-}N_4)$	1.323	1.316	0.006	0.002	1.30
$r(N_1{-}N_2)$	1.344	1.355	−0.005	−0.003	1.33
$r(N_2{-}N_3)$	1.319	1.293	0.003	0.001	1.33
$r(N_3{-}N_4)$	1.361	1.372	−0.001	−0.003	1.30
$r(C_5{-}H_5)$	1.073	1.081	0.001	0.001	0.98
$r(N_1{-}H_1)$	1.005	1.012	0.005	0.008	1.10
$\angle N_1C_5N_4$	108.34	108.70	−0.15	0.38	106.7
$\angle C_5N_1N_2$	109.42	108.54	0.31	−0.26	108.5
$\angle C_5N_4N_3$	105.88	105.47	−0.13	−0.26	109.4
$\angle N_1N_2N_3$	105.47	106.00	1.65	0.26	107.6
$\angle N_4N_3N_2$	110.90	111.30	−0.05	−0.12	107.8
$\angle H_5C_5N_1$	124.88	124.80	−0.39	−0.14	115.0
$\angle H_1N_1C_5$	130.32	131.18	−0.93	−0.80	120.0

[a] MP2/6-311G(2d,2p) values. [b] QCISD/6-31G* values. [c] Change from the gas phase to a dielectric medium of $\epsilon = 40$ ($a_0 = 3.0$ Å, HF/6-31G*). [d] Change from monomer to dimer (HF/6-31G*). [e] Taken from ref 2.

Table VII. Optimized Structural Parameters for the Transition Structures of Tetrazole

	gas phase		solution[a,b]	
parameter	HF/6-31G*	MP2/6-31G*	$\epsilon = 2$	$\epsilon = 40$
	T.S. (**4**): $\mathbf{1} \rightarrow \mathbf{2}$			
$r(C_5{-}N_1)$	1.319	1.347	0.000	−0.001
$r(C_5{-}N_4)$	1.318	1.339	0.001	0.002
$r(N_1{-}N_2)$	1.393	1.449	−0.001	−0.003
$r(N_2{-}N_3)$	1.284	1.335	−0.001	−0.002
$r(N_3{-}N_4)$	1.293	1.340	0.000	−0.001
$r(C_5{-}H_5)$	1.068	1.080	0.000	0.000
$r(N_1{\cdots}H_1)$	1.249	1.262	0.002	0.005
$r(N_2{\cdots}H_1)$	1.302	1.246	0.002	0.006
$\angle N_1C_5N_4$	111.39	112.90	−0.07	−0.20
$\angle C_5N_1N_2$	103.07	102.17	0.08	0.21
$\angle C_5N_4N_3$	106.79	106.84	0.02	0.05
$\angle N_1N_2N_3$	109.42	108.25	−0.05	−0.13
$\angle N_4N_3N_2$	111.94	109.40	0.01	0.03
$\angle H_1N_1C_5$	116.59	121.92	0.12	0.30
$\angle H_5C_5N_1$	123.98	123.05	0.00	−0.01
$\angle N_1H_1N_2$	68.61	70.58	−0.21	−0.35
$\tau N_2N_1C_5N_4$	−1.98	−3.54	−0.10	−0.25
$\tau N_3N_4C_5N_1$	4.07	6.47	0.07	0.35
$\tau H_5C_5N_1N_2$	179.65	180.03	−0.17	−0.43
$\tau H_1N_1C_5N_4$	−59.00	−58.72	−0.12	−0.31
$\tau H_1N_2N_3N_4$	54.29	64.47	−0.08	−0.21
	T.S. (**5**): $\mathbf{1} \rightarrow \mathbf{3}$			
$r(C_5{-}N_1)$	1.387	1.444	−0.001	−0.002
$r(C_5{-}N_4)$	1.333	1.348	0.001	0.004
$r(N_1{-}N_2)$	1.302	1.337	0.000	0.000
$r(N_2{-}N_3)$	1.289	1.347	0.001	0.002
$r(N_3{-}N_4)$	1.284	1.337	−0.001	−0.002
$r(C_5{-}H_5)$	1.070	1.084	0.000	0.001
$r(N_1{\cdots}H_5')$	1.302	1.305	0.002	0.006
$r(C_5{\cdots}H_5')$	1.249	1.266	0.002	0.005
$\angle N_1C_5N_4$	108.89	109.96	−0.06	−0.16
$\angle C_5N_1N_2$	104.29	103.21	0.09	0.22
$\angle C_5N_4N_3$	105.34	105.59	0.01	0.04
$\angle N_1N_2N_3$	108.24	110.19	0.00	0.00
$\angle N_4N_3N_2$	110.31	110.90	−0.03	−0.08
$\angle H_5C_5N_1$	123.52	122.48	0.06	0.15
$\angle H_5'N_1C_5$	56.01	54.58	−0.02	−0.05
$\angle N_1H_5'C_5$	65.42	68.29	−0.15	−0.27
$\tau N_2N_1C_5N_4$	−2.87	−2.78	0.03	0.07
$\tau N_3N_4C_5N_1$	1.13	0.53	−0.04	−0.10
$\tau H_5C_5N_1N_2$	−168.48	−166.90	−0.12	−0.32
$\tau H_5'N_1C_5N_4$	−104.48	−105.99	−0.27	−0.43
$\tau H_5'C_5H_5N_4$	−144.23	−137.02	0.05	0.13

[a] SCRF calculations ($a_0 = 3.45$ Å). [b] Change from the gas phase to solution (HF/6-31G*).

We are not aware of any theoretical study dealing with tautomerism of tetrazole in the liquid phase. In this study, we have employed the self-consistent reaction field (SCRF) theory[13] to examine the solvent effect on this tautomeric equilibrium. The calcualted dipole moments of 1*H*- and 2*H*-tetrazole at the MP2/6-311+G** level are 5.58 and 2.43 D, respectively (Table III), in reasonable agreement with the gas-phase experimental values (5.30 and 2.19 D).[2] With this large difference in dipole moment, one would expect a differential solvent stabilization in solution. For instance, in a nonpolar solvent of $\epsilon = 2$, 1*H*-tetrazole

Table VIII. Calculated Vibrational Frequencies (cm^{-1}) and Infrared Intensities ($km\ mol^{-1}$) of Tetrazole Isomers[a]

		frequency			intensity		
		$\epsilon = 1$		$\epsilon = 40$[b]	$\epsilon = 1$		$\epsilon = 40$[c]
		HF	MP2	HF	HF	MP2	HF
		1H-Tetrazole (**1**)					
A′	ν_1	1093	972	7	2	3	2
	ν_2	1115	1014	2	2	4	1
	ν_3	1182	1097	17	24	31	−2
	ν_4	1204	1121	7	36	10	19
	ν_5	1262	1160	4	19	17	8
	ν_6	1429	1207	−2	1	2	2
	ν_7	1549	1280	−4	38	2	16
	ν_8	1629	1495	2	11	29	2
	ν_9	1722	1507	−4	26	8	12
	ν_{10}	3496	3351	0	0	2	4
	ν_{11}	3925	3662	−35	139	115	98
A″	ν_{12}	623	613	50	131	73	1
	ν_{13}	753	700	11	7	17	15
	ν_{14}	815	737	4	9	16	5
	ν_{15}	1010	816	21	9	31	−1
		2H-Tetrazole (**2**)					
A′	ν_1	1110	1001	0	23	11	5
	ν_2	1144	1039	2	28	14	8
	ν_3	1232	1119	3	27	22	7
	ν_4	1284	1162	3	37	23	8
	ν_5	1328	1234	2	6	0	3
	ν_6	1439	1248	−4	8	5	3
	ν_7	1474	1349	1	16	15	4
	ν_8	1591	1417	−1	11	7	3
	ν_9	1741	1516	0	5	3	1
	ν_{10}	3502	3353	−1	1	0	1
	ν_{11}	3919	3648	−15	153	122	71
A″	ν_{12}	671	622	23	58	38	4
	ν_{13}	786	715	−2	61	30	10
	ν_{14}	821	744	3	26	57	4
	ν_{15}	1022	878	−4	11	17	0
		5H-Tetrazole (**3**)					
A_1	ν_1	763	325	3	1	1	0
	ν_2	1059	763	−2	10	12	7
	ν_3	1091	879	−2	5	26	2
	ν_4	1573	1473	−8	13	9	13
	ν_5	1839	1826	−3	0	7	1
	ν_6	3272	3155	0	0	0	3
A_2	ν_7	653	418	4	0	0	0
	ν_8	1290	1202	0	0	0	0
B_1	ν_9	443	350	1	9	6	1
	ν_{10}	1036	905	−7	21	6	3
	ν_{11}	3327	3241	0	0	0	0
B_2	ν_{12}	1934	279	−2	9	56	1
	ν_{13}	1015	729	−2	7	21	5
	ν_{14}	1112	1314	1	37	11	7
	ν_{15}	1454	1899	1	0	12	0

[a] Unscaled values; 6-31G* basis set. [b] Frequency shift from the gas phase to solution. [c] Intensity change from the gas phase to solution.

is computed to have a larger stabilization energy (10 kJ mol^{-1}) than *2H*-tetrazole (2 kJ mol^{-1}). Thus, both tautomeric forms are predicted to lie close in energy in nonpolar media. This differential solvent stabilization effect is more pronounced in a polar medium of $\epsilon = 40$ (Table III). As a consequence, a reversal of stability is predicted for the tetrazole system in a polar dielectric medium. These results are consistent with experimental observations of *1H*-tetrazole in condensed phases.[2,3] Note that there is a substantial enhancement of the dipole moment (by 1 D) of the *1H* tautomer in going from the gas phase to a polar medium (Table III).

Previous SCRF studies have shown that the difference between MP2 and a higher level of electron correlation treatment (such as QCISD) is relatively constant in going from the gas phase to solutions.[15c,24] Here, we have calculated the QCISD − MP2 corrections for the energy difference between **1** and **2** with ϵ = 1, 2, and 40, using the 6-31G* basis set; the computed ΔE values are 8.5, 8.6, and 8.6 kJ mol^{-1}, respectively. This again demonstrates the validity of this approximation. Hence, for the tetrazole system considered here, we have assumed that the energy difference between MP2 and QCISD(T) remains constant in going from vacuo to solution. In other words, the "solution" ΔE values at the QCISD(T) level were estimated from the gas-phase QCISD(T) values together with solvation energies calculated at the MP2 level (Table IV). We have calculated the tautomerization free energy (ΔG) of *1H*-tetrazole in the gas phase and in solutions (Table IV). The enthalpy of tautomerization reaction, ΔH, was calculated from ΔE, Δ(ZPVE), and $\Delta(H - H_0)$; and the final ΔG value was computed from the equation $\Delta G = \Delta H - T\Delta S$, where ΔS is the entropy change. The calculated free energies of tautomerization for *1H*-tetrazole are −7, 1, and 12 kJ mol^{-1} for ϵ = 1, 2, and 40, respectively. The corresponding tautomeric equilibrium constants (K_T) of *1H*-tetrazole were calculated from the expression $\Delta G = -RT \ln K_T$. The computed log K_T values are 1.30, −0.10, and −2.12 for ϵ = 1, 2, and 40, respectively. Hence, our results suggest that the tautomeric equilibrium of *1H*-tetrazole is strongly dependent on solvent polarity. In polar dielectric media, tetrazole is predicted to exist predominantly as the *1H* tautomer, in contrast to the preference of the *2H* tautomer in the gas phase. These computational results are consistent with the experimental finding that tetrazole exists predominantly as the *1H* tautomer in polar solvents.[3a,d] In particular, tetrazole is found to exist exclusively as the *1H* form in DMSO solution.[3a] In summary, the reversal of tautomeric equilibrium of tetrazole in solution can be attributed to solvation.

It is worthwhile to note that the free energy of solvation calculated at the MP2 level is satisfactorily reproduced by the Hartree–Fock calculations. For instance, the calculated solvation free energies of *1H*-tetrazole in a dielectric medium of $\epsilon = 40$ are 26 and 27 kJ mol^{-1} at the HF/6-31G* and HF/6-311+G** levels, respectively, which compare well to our best estimate of 25 kJ mol^{-1} at the MP2/6-311+G** level (Table III). However, a higher-level treatment of electron correlation, such as QCISD, is essential for a prediction of the absolute free energy in solution. A similar finding has been reported for the tautomeric equilibrium of 2-pyridone.[15c]

Equilibrium Structures

To the best of our knowledge, there are no published experimental data on the structures of *1H*- (**1**), *2H*- (**2**), and *5H*-tetrazole (**3**) in the gas phase. However, structural data for *1H*-tetrazole in the solid state are available.[2] The molecular structures of **1** and **2** have been examined by several semiempirical and ab

Table IX. Calculated Electron Populations of Tetrazole Isomers[a,b]

1H-tetrazole (**1**)			*2H*-tetrazole (**2**)			*5H*-tetrazole (**3**)		
atom	$\epsilon = 1$	$\epsilon = 40$[c]	atom	$\epsilon = 1$	$\epsilon = 40$[c]	atom	$\epsilon = 1$	$\epsilon = 40$[c]
N_1	8.075	−0.001	N_1	7.817	−0.015	N_1	7.448	−0.006
N_2	7.043	0.004	N_2	7.432	−0.006	N_2	7.034	0.026
N_3	7.038	0.045	N_3	7.015	0.006	N_3	7.036	0.026
N_4	7.920	0.016	N_4	7.743	0.019	N_4	7.445	−0.006
C_5	4.528	0.000	C_5	4.574	−0.001	C_5	5.135	−0.001
H_1	0.477	−0.026	H_2	0.469	−0.010	H_5	0.952	−0.020
H_5	0.932	−0.034	H_5	0.949	0.006	H_5'	0.952	−0.020
total	36.004	−0.001	total	35.999	−0.001	total	36.002	0.000

[a] HF/6-31+G**//HF/6-31G* wavefunctions. [b] Atom labels are illustrated in Figure 1. [c] Change from the gas phase to solution.

initio calculations.[7] The best theoretical estimates to date correspond to those reported by Mazurek and Osman at the HF/6-31G level.[7g] Here we have carried out geometry optimizations for all three isomers of tetrazole with a slightly larger 6-31G* basis set at both the Hartree–Fock and MP2 levels. All equilibrium structures were confirmed to be planar by the vibrational frequency calculations, which gave all real frequencies. Comparison of our HF/6-31G* optimized structural parameters with those calculated at the HF/6-31G level shows that the optimized geometries are significantly affected by the inclusion of d-polarization on C and N atoms. All the C–N and N–N bond lengths calculated at the HF/6-31G* level are 0.02–0.03 Å longer. Geometry optimizations with the inclusion of electron correlation (MP2/6-31G*) are reported for the first time for 1*H*- and 2*H*-tetrazole. Large structural changes are observed in going from the HF to MP2 level (Table V). The calculated bond lengths at the MP2 level are considerably longer (by 0.011–0.069 Å) than the corresponding Hartree–Fock values. In particular, the skeletal bond lengths are calculated to be more delocalized at the correlated level. Therefore, geometry optimization with the inclusion of electron correlation should be important for more accurate prediction. Geometry optimizations at the MP2 level generally provide good agreement with experimental data.[16] However, for 1*H*-tetrazole (**1**), the calculated structural parameters (MP2/6-31G*) are significantly different from the solid-state experiment values (Tables V and VI).[2] For instance, the calculated N_3–N_4 bond length is 0.032 Å longer and the calculated $H_1N_1C_5$ bond angle is 10° larger than the experimental values. Structural parameters obtained at higher levels of theory, MP2/6-311G-(2d,2p) and QCISD/6-31G* (Table VI), are similar to those obtained at the MP2/6-31G* level. The discrepancy between the calculated and observed molecular geometry may be attributed to the fact that 1*H*-tetrazole in the solid state is aggregated.[2] To examine this possibility, we have considered the effect of medium on the structure of this polar compound by two different approaches. First, we have employed the SCRF method to calculate the structure of 1*H*-tetrazole in the presence of a reaction field ($\epsilon = 40$). Since tetrazole is more densely packed in the solid state than in the liquid phase, a smaller cavity radius ($a_0 = 3.0$ Å) is used for the optimization. Second, we have investigated the structural change of the 1*H* tautomer in a hydrogen-bonding environment. The previous X-ray study has shown that intermolecular hydrogen bonding is important in the crystalline state of 1*H*-tetrazole.[2] The hydrogen atom (H_1) on N_1 form a hydrogen bond with the N_4 atom of an adjacent molecule. The calculated structural changes by these two approaches, compared to the optimized (monomer) geometry in vacuo, are collected in Table VI. Both methods lead to similar changes in molecular structure. For example, the calculated C_5–N_4 and N_1–H_1 bond lengths are found to be altered significantly by 0.006–0.008 Å. However, this calculated medium effect, both in magnitude and direction, cannot account for the inconsistency between the calculated results and the solid-state geometry. It is interesting to note that the measured C–H bond length is even shorter than the N–H distance (by 0.12 Å).[2] We are planning to reexamine the crystal structure of 1*H*-tetrazole.

The calculated changes in structure in going from the gas phase to solutions are given in Table V. As one might have expected, the introduction of a solvent reaction field has little effect on the calculated geometry of 2*H*- and 5*H*-tetrazole. On the other hand, a larger change in molecular geometry is predicted for the more polar 1*H* form **1**. The calculated C_5–N_4, N_1–N_2, and N_1–H_1 bond lengths are found to be altered by 0.003–0.004 Å in going from the gas phase to a solvent of dielectric constant 40. These changes, lengthenings of C_5–N_4 and N_1–N_1 bonds and shortening of N_1–N_2 bonds, correspond to a small increase in the weight of the dipolar resonance structure.

The calculated skeletal bond lengths (1.321–1.362 Å, MP2/6-31G*) for both 1*H*- (**1**) and 2*H*-tetrazole (**2**) (Table V) lie between those of isolated single and double bonds, indicating that the molecules are aromatic. For comparison, the experimental C=N bond length is 1.273 Å in methyleneimine ($H_2C{=}NH$), and the N—N distances in H—N=N—H and H_2N—NH_2 are 1.252 and 1.449 Å, respectively.[27] These results clearly indicate that the lone pair electrons at N_1 in **1** and at N_2 in **2** are delocalized in planar five-center 6π-electron aromatic systems, similar to pyrrole. We have also optimized the structure of the tetrazole anion **6**, and, as expected, it is found to have "aromatic" bond lengths, 1.345–1.359 Å (Table V).

5*H*-Tetrazole (**3**) is planar and has localized single and double bonds, as evidenced by the long N_1–C_5 bond length (1.442 Å) and the short N_1–N_2 bond length (1.206 Å) (Table V). At the Hartree–Fock level, **3** has a cyclic structure, $r(N_2–N_3) = 1.472$ Å and $\angle N_1N_2N_3 = 109°$. Inclusion of electron correlation at the MP2 level changes the picture dramatically. The MP2/6-31G* level predicts an acyclic structure, $r(N_2–N_3) = 2.191$ Å and $\angle N_1N_2N_3 = 95°$ (Figure 3). Explicit calculation of vibrational frequencies at the MP2/6-31G* level confirms that this acyclic structure is a local minimum on the MP2/6-31G* potential energy surface. Larger-basis-set optimization at the MP2/6-311G(2d,2p) level still leads to an acyclic geometry (Figure 3). However, higher levels of electron correlation treatment, MP3/6-31G* and QCISD/6-31G*, cause a reversal back to the expected cyclic geometry (Figure 3). Therefore, the QCISD/6-31G* optimized geometry (instead of the MP2/6-31G* geometry) was used for the higher-level energy calculation in vacuo. In the gas phase, 5*H*-tetrazole (**3**) is calculated to be less stable than the 1*H* (**1**) and 2*H* (**2**) tautomers by 82 and 90 kJ mol^{-1}, respectively, thereby explaining the nonobservation of **3** to date. These values are similar to the resonance energy found for pyrrole, ca. 105 kJ mol^{-1}.[28]

[1,2] and [1,5] Hydrogen Shifts

The transition structure **4** for the symmetry-allowed hydrogen shift[11] from 1*H*- (**1**) to 2*H*-tetrazole (**2**) is shown in Figure 2. Except for the N_1–N_2 bond length (1.449 Å), the skeletal bond lengths are "aromatic", 1.335–1.347 Å (MP2/6-31G*, Table VII). The skeletal framework is unlike that of the tetrazole anion (**6**) (Table V), in which all the bond lengths correspond to a delocalized, aromatic system. Instead, the five heavy atoms and the migrating hydrogen atom (H_1) form an aromatic 6π-electron monocycle[29] with a small perturbation of the N_1–N_2 overlap. The heavy atoms and atom H_5 lie virtually in the same plane. The migrating hydrogen atoms is moving 59° out of plane ($\tau H_1N_1C_5N_4$), and the "transfer angle" ($\angle N_1H_1N_2$) is 71°. The energy barrier for the rearrangement of **1** to **2** is calculated to be 207 kJ mol^{-1} in the gas phase (at the QCISD(T)/6-311+G-(2d,2p) + ZPVE level). This value is significantly smaller than the previously reported semiempirical value of 290 kJ mol^{-1}.[7d] A similar hydrogen "transfer angle" (68°) and out-of-plane angle (79°) were predicted for the [1,5] hydrogen migration in cyclopentadiene (at the HF/3-21G level).[29] Since transition structure **4** is less polar than 1*H*-tetrazole (by 2.3 D), the calculated barrier for the isomerization of **1** to **2** should increase in a medium of high dielectric constant. Indeed, in a polar solvent of $\epsilon = 40$, the energy barrier for rearrangement of **1** to **2** is predicted to be 12 kJ mol^{-1} higher than the gas-phase value (Table IV). Introduction of a dielectric medium has little effect on the optimized transition structure **4**, except for the distance of the migrating hydrogen (Table VII).

---

(27) Harmony, M. D.; Laurie, V. W.; Kuczkowski, R. L.; Schwendeman, R. H.; Ramsay, D. A.; Lovas, F. L.; Lafferty, W. J.; Maki, A. G. *J. Phys. Chem. Ref. Data* **1979**, *8*, 619.

(28) (a) Streitwieser, A., Jr.; Heathcock, C. H. *Introduction to Organic Chemistry*; Macmillan Publishing Co., Inc.: New York, 1981. (b) March, J. *Advanced Organic Chemistry*; Wiley-Interscience: New York, 1985. (c) Morrison, R. T.; Boyd, R. N. *Organic Chemistry*; Allyn and Bacon, Inc.: New York, 1987. (d) Jackson, A. H. *Comprehensive Organic Chemistry*; Pergamon Press: New York, 1979; Vol. 4.

(29) (a) Rondan, N. G.; Houk, K. N. *Tetrahedron Lett.* **1984**, *2519*. (b) Kahn, S. D.; Hehre, W. J.; Rondan, N. G.; Houk, K. N. *J. Am. Chem. Soc.* **1985**, *107*, 8291.

(30) For example, see: (a) Meier, H.; Zeller, K.-P. *Angew. Chem., Int. Ed. Engl.* **1975** *14*, 32. (b) Georgian, V.; Boyer, S. K.; Edwards, B. *J. Org. Chem.* **1980**, *45*, 1686. (c) Battye, P. J.; Jones, D. W. *J. Chem. Soc., Chem. Commun.* **1984**, 1458. (d) Spangler, C. W. *Chem. Rev.* **1976**, *76*, 187.

The transition structure **5** for the [1,5] hydrogen migration from 1*H*- (**1**) to 5*H*-tetrazole (**3**) is displayed in Figure 2. As with transition structure **4**, the five skeletal atoms and the migrating hydrogen in **5** form an aromatic 6π-electron monocycle. The skeletal bond lengths are in the range of 1.337–1.348 Å, while the N_1–C_5 bond length is longer (1.444 Å) (Table VII). The C_5 atom is significantly pyramidalized to maintain bonding with the migrating hydrogen (H_5'). Atom H_5 rotates out of plane by about 13° ($\tau H_5C_5N_1N_2$) in order to maximize overlap between C_5 and the incoming migrating hydrogen. The heavy atoms are almost coplanar. The migrating hydrogen "transfer angle" is 68° ($\angle C_5H_5'N_1$), fairly close to that found for **4**, and it is moving about 61° ($\tau H_5'C_5N_4N_3$) out of plane. The calculated energy barrier for the rearrangement **1** to **3** in the gas phase is 232 kJ mol^{-1}, 25 kJ mol^{-1} larger than that for the [1,2] hydrogen shift from **1** to **2**. Conversely, the energy barrier for the rearrangement of **3** to **1** is 150 kJ mol^{-1}. These results indicate that **3**, although less stable than isomers **1** and **2** by about 85 kJ mol^{-1}, is separated by a significant enthalpic barrier and is therefore a good candidate for experimental observation. Thus, a suitably substituted 5*H*-tetrazole with a poor migrating substituent[31] is a worthy topic for future research. Furthermore, our computational results suggest that a [1,5] hydrogen shift from 1*H*- (**1**) to 5*H*-tetrazole (**3**) is as competitive as the [1,2] hydrogen shift from **1** to **2**. Therefore, [1,5] hydrogen shift of 1*H*-tetrazole to the unknown 5*H* tautomer **3** is perfectly possible, e.g., in gas-phase pyrolysis reactions leading to diazo compounds.[9,30] Due to a differential stabilization of **1** over **5** in solution, the energy required for the isomerization of **1** to **3** in a polar solvent of $\epsilon = 40$ is calculated to be 18 kJ mol^{-1} higher than that in vacuo (Table IV).

The activation energies required for the direct hydrogen transfer from **1** to **2** and from **1** to **3** are predicted to be relatively high (207 and 232 kJ mol^{-1}, respectively) compared to the activation energies required for [1,5] hydrogen shift in pentadeuteriocyclopentadiene and 5-methylcyclopentadiene (147 and 105 kJ mol^{-1}, respectively) determined from kinetic experiments.[31] Note that there have recently been some suggestions that hydrogen shifts in nitrogen-containing species may be facilitated by water-assisted double-proton transfer as well as dimerization-assisted double-proton transfer relative to the direct proton transfer.[32]

Vibrational Frequencies and Infrared Spectra

To facilitate future characterization of tetrazole tautomers, we have reported the infrared spectra of all three isomers, calculated at the HF/6-31G* and MP2/6-31G* levels. As can be seen in Table VIII, the characteristic features of the spectra of 1*H*- (**1**) and 2*H*-tetrazole (**2**) are the strong absorption bands of the N–H stretching (ν_{11}) and bending (ν_{12}). IR absorption bands between 1000 and 1100 cm^{-1} have been reported for many tetrazole derivatives.[1] The vibrational frequencies in this region, ν_3, ν_4, and ν_5 for **1**, can be assigned to the cyclic C—N═N and N—N═N groups. Since **1** and **2** are calculated to have similar IR spectra, it may not be straightforward to use IR spectroscopy to differentiate between these two tautomeric forms. Significant frequency shifts upon solvation are generally observed for N–H stretching bands. For 1*H*-tetrazole, a red shift of 35 cm^{-1} is predicted in going from the vapor phase to a polar medium of $\epsilon = 40$. A significant frequency shift (50 cm^{-1}) is also calculated for the N_1–H_1 bending (ν_{12}) mode of **1**. Smaller changes in vibrational frequencies in going from vacuo to solution are computed for the less polar 2*H*- and 5*H*-tetrazole. The infrared intensities of most absorption bands are calculated to become more intense in going from the gas phase to solution.

Solvent Effect on Charge Distribution

In previous solvent effect studies,[13,15] charge distributions of dipolar compounds were often found to be altered significantly by a solvent reaction field. In view of the large N–H bond dipole, one might anticipate that it would become polar in going from the gas phase to solution. We have examined the charge distributions of all tetrazole isomers in both the gas phase and in a polar medium ($\epsilon = 40$) using Bader's theory of atoms in molecules.[25] As can be seen in Table IX, the electron population at the N–H hydrogen does decrease in going from the gas phase to solution, and, as expected, the effect is larger for the more polar 1*H*-tetrazole (**1**). However, the change at the N–H hydrogen does not come from the neighboring nitrogen but instead comes from another skeletal nitrogen (e.g., N_3 for **1**). In other words, the charge distribution in solution is more delocalized than one would have expected from the dipolar resonance picture. Interestingly, the C–H hydrogen in 1*H*-tetrazole also experiences a significant decrease in electron population (Table IX). Overall, it can be seen that the electron density is transferred from the hydrogens to the skeletal nitrogen atoms, which leads to a larger degree of charge separation in the presence of a solvent reaction field. The calculated changes on charge distributions are in accord with the changes in dipole moments, molecular geometries, and vibrational frequencies in going from the gas phase to solution.

Conclusions

Several interesting points have been revealed by this study:

(1) The 1*H*-tetrazole (**1**)/2*H*-tetrazole (**2**) equilibrium is calculated to be medium dependent. In the gas phase, 2*H*-tetrazole is predicted to be the dominant form. In nonpolar solvents, both tautomers are very close in energy. However, in solvents of high dielectric constant and in the solid state, the tautomeric equilibrium is shifted in favor of the more polar 1*H* tautomer. These results are in good accord with experimental observations. The free energy of tautomerization of 1*H*-tetrazole in the gas phase ($\epsilon = 1$) and in nonpolar ($\epsilon = 2$) and polar media ($\epsilon = 40$) are predicted to be −7, 1, and 12 kJ mol^{-1}, respectively.

(2) The stabilities of **1** and **2** can be ascribed to their aromatic characters with delocalization of the lone pair of electrons of the saturated nitrogen atom into the 5-membered ring to form 6π-electron aromatic systems. Isomerization of **1** to **2** is calculated to be have an energy barrier of 207 kJ mol^{-1} in the gas phase.

(3) 5*H*-Tetrazole (**3**) is predicted to be less stable than either **1** or **2** by about 85 kJ mol^{-1}, principally due to its nonaromatic character. However, rearrangement of **3** to **1** requires an energy barrier of 232 kJ mol^{-1}, slightly larger than the activation energy required for the isomerization of **1** to **2**. Thus, the unknown 5*H*-tetrazole should be an experimentally accessible species.

(4) Geometry optimizations at the correlated level are reported for the first time for the equilibrium structures of tetrazole. The calculated structural parameters of 1*H*-tetrazole are significantly different from the solid-state experimental values. For 5*H*-tetrazole, inclusion of electron correlation leads to a dramatic change in the molecular structure. While calculations at the MP3 and QCISD levels predict a reasonable cyclic structure (**3a**), calculations at the MP2 level lead to an unexpected acyclic structure (**3b**).

Acknowledgment. We thank Dr. Douglas J. Brecknell for technical assistance and the Australian Research Council (ARC) for financial support. M. W. Wong thanks ARC for an Australian Research Fellowship.

---

[31] (a) Roth, W. R. *Tetrahedron Lett.* **1964**, *1009*. (b) McLean, S.; Haynes, P. *Tetrahedron* **1965**, *21*, 2329. (c) Roth, W. R.; Konig, J. *Justus Liebigs Ann. Chem.*, **1966**, *699*, 24. (d) Roth, W. R. *Chimia* **1966**, *229*, 20.

[32] Nguyen, K. A.; Gordon, M. S.; Truhlar, D. G. *J. Am. Chem. Soc.* **1991**, *113*, 1596.